® Postepy Hig Med Dosw (online), 2015; 69: 1259-1267
e-ISSN 1732-2693

www.phmd.pl
Original Article

Received: 2014.12.22
Accepted: 2015.08.06
Published: 2015.12.01

Expression of cyclin A in A549 cell line after treatment with arsenic trioxide*

Ekspresja cykliny A w linii komórkowej A549 po traktowaniu trójtlenkiem arsenu

Agnieszka Żuryń[1, A, B, D, E, F, G], **Adrian Krajewski**[1, B, D, E, F], **Anna Litwiniec**[2, C, D, E], **Anna Klimaszewska–Wiśniewska**[1, B], **Alina Grzanka**[1, A, G*]

[1] Department of Histology and Embryology, Nicolaus Copernicus University in Torun, Collegium Medicum in Bydgoszcz, Faculty of Medicine, Karlowicza 24, 85-092 Bydgoszcz, Poland
[2] Plant Breeding and Acclimatization Institute – National Research Institute, Bydgoszcz Research Center, Department of Genetics and Breeding of Root Crops, Laboratory of Biotechnology, Powstanców Wielkopolskich 10, 85-090 Bydgoszcz, Poland

Authors' Contribution:
A Study Design
B Data Collection
C Statistical Analysis
D Data Interpretation
E Manuscript Preparation
F Literature Search
G Funds Collection

Summary

Background: Arsenic trioxide (ATO) is an effective drug used in acute promyelocytic leukemia (AML). Many reports suggest that ATO can also be applied as an anticancer agent for solid tumors in the future. The influence of arsenic trioxide on the expression of different cell cycle regulators is poorly recognized. The purpose of the current study is to investigate how arsenic trioxide affects cyclin A expression and localization in the A549 cell line.

Materials and methods: Morphological and ultrastructural changes in A549 cells were observed using light and transmission electron microscopes. Cyclin A localization was determined by immunofluorescence. Image-based cytometry was applied to evaluate the effect of arsenic trioxide on apoptosis and the cell cycle. Expression of cyclin A mRNA was quantified by real-time PCR.

Results: After treatment with arsenic trioxide, increased numbers of cells with cytoplasmic localization of cyclin A were observed. The doses of 10 and 15 μM ATO slightly reduced expression of cyclin A mRNA. The apoptotic phenotype of cells was poorly represented, and the Tali image-based cytometry analysis showed low percentages of apoptotic cells. The A549 population displayed an enriched fraction of cells in G0/G1 phase in the presence of 5μM ATO, whereas starting from the higher concentrations of the drug, i.e. 10 and 15 μM ATO, the G2/M fraction was on the increase.

Discussion: Low expression of cyclin A in the A549 cell line may constitute a potential factor determining arsenic trioxide resistance. It could be hypothesized that the observed alterations in cyclin A expression/distribution may correlate well with changes in cell cycle regulation in our model, which in turn determines the outcome of the treatment.

Key words: cyclin A • A549 cell line • arsenic trioxide (ATO) • cell death • cell cycle

*The work was supported by the Nicolaus Copernicus University, Collegium Medicum (grant no. 895).

Full-text PDF: http://www.phmd.pl/fulltxt.php?ICID=1184239

Word count: 3610
Tables: –
Figures: 6
References: 30

Author's address: Agnieszka Żuryń, Ph.D., Nicolaus Copernicus University, Collegium Medicum in Bydgoszcz, Department of Histology and Embryology, Karłowicza 24, Bydgoszcz 85-092, Poland; e-mail: azuryn@cm.umk.pl

Introduction

Arsenic trioxide (ATO) is an effective drug for acute promyelocytic leukemia (APL). The mechanism of action of As_2O_3 in APL mainly involves interaction with the fusion protein PML-RARα, which is characteristic of APL [19]. Scientific data indicate that arsenic trioxide can be an efficient therapeutic agent for the treatment of solid tumors. Apart from its impact on PML-RARα, arsenic trioxide affects a lot of molecular pathways, the activation or downregulation of which can induce apoptosis. In addition, ATO can induce cell cycle arrest in G0/G1 and G2/M phases. Triggering another type of cell death, autophagy, has also been reported [3,20,28]. Despite the efforts to investigate arsenic trioxide's mechanism of action, specific interactions between ATO and its molecular targets remain to be elucidated. The influence of arsenic trioxide on cell cycle regulators is poorly investigated. Cyclins are proteins that are responsible for cell cycle transition in a time-dependent coordinated manner. Each cyclin phosphorylates its respective cyclin-dependent kinase (CDK), which in turn induces a cascade of events and progression through the cell cycle. During S phase, cyclin A binds to CDK2 and determines the accuracy of the replication process. On the turn of G2 and M phases, cyclin A activates CDK1 and with participation of MPF complex (cyclin B/CDK1/p34) controls the G2/M transition and mitosis initiation. Cyclin A localizes predominantly in the nucleus during S phase, where it phosphorylates CDC6, which results in its inactivation and degradation, thus preventing interruption of the replication [4]. At the G2/M transition, cyclin A is responsible for accumulation and activation of CDK1/cyclin B complex [14]. Additionally, cyclin A takes part in chromatin condensation and nuclear envelope breakdown [10-11]. Cyclin A controls transition from prophase to metaphase, affecting kinetochore microtubules stabilization, and assures optimal time of prophase duration for faithful chromosome segregation [17]. The cyclin A/CDK1 complex phosphorylates APC protein at early M phase, which is indispensable for proper orientation of the mitotic spindle [2]. Overexpression or depleted levels of cyclin A have been found in several types of human tumors. It has been proven that arsenic trioxide is able to change the expression profile of cell cycle and apoptosis-related proteins in the A549 cell line; however, its impact on cyclin expression is poorly known [26]. The A549 cell line used in the current study was initiated in 1972 through explant culture of lung carcinomatous tissue from a 58-year-old Caucasian male. A549 cells could synthesize lecithin with a high percentage of desaturated fatty acids utilizing the cytidine diphosphocholine pathway. The cells are positive for keratin in immunoperoxidase staining [9,21]. The A549 cells originate from type II alveolar epithelium and display expression of several cytochrome P450 (CYP) enzymes, which undergo differential regulation in response to xenobiotics. This non-small cell lung carcinoma cell line is therefore believed to constitute a perfect model for studies concerning the pulmonary CYP system [7,15]. In the current study we evaluated the influence of arsenic trioxide on cyclin A expression and localization in the A549 cell line. Moreover, we determined morphological and ultrastructural changes in A549 cells after ATO treatment. We also investigated ATO-induced apoptosis and cell cycle arrest. Our results suggest that the A549 cell line may display a low level of cyclin A expression, which however may be differentially regulated depending on the cell cycle arrest resulting from the ATO dose used for the treatment.

Materials and Methods

Cell culture

The human non-small cell lung carcinoma cell line A549 was kindly provided by P. Kopiński, Ph.D. (Department of Gene Therapy, Ludwik Rydygier Collegium Medicum in Bydgoszcz, Nicolaus Copernicus University in Toruń, Poland). The cells were cultured in monolayers at 37°C in a CO_2 incubator in Dulbecco's Modified Eagle Medium (DMEM) (Lonza, Verviers, Belgium) with the addition of 10% fetal bovine serum (FBS; Gibco/Life Technologies, Carlsbad, CA, USA) and 50 µg/ml of gentamycin (Sigma-Aldrich, St. Louis, MO, USA). Arsenic trioxide (Adriblastin PFS; Pharmacia Italia S.p.A., Pfizer Group) was diluted in sterile water and was added to the cell culture at appropriate doses. Twenty-four hours after seeding, the cells were exposed to ATO (5, 10 and 15 µM) for 24 h.

Light microscopy

The light microscope was applied to investigate morphological alternations in the A549 cell line. Cells were fixed in 4% paraformaldehyde, then washed three times for 5 minutes with PBS and five times for 30 seconds with

distilled water. The cells were stained with Mayer's hematoxylin, then washed three times with tap water for 5 minutes. The cells were incubated for 10 minutes with PBS and then mounted with Aqua-Poly/Mount (Polysciences Warrington, PA, USA). The preparations were analyzed in an Eclipse E800 microscope (Nikon) with the NIS-Elements image analysis system and a CCD camera (DS-5Mc-U1; Nikon).

Transmission electron microscopy

Conventional electron microscopy was used to visualize A549 cell morphology at the ultrastructural level. The cells were washed with sodium cacodylate buffer and fixed in 3.6% glutaraldehyde (pH 7.2, Polysciences, Warrington, PA, USA) (30 min, room temperature [RT]). After washing in 0.1 M sodium cacodylate buffer (pH 7.4; Roth, Karlsruhe, Germany), the cells were postfixed in 1% buffered OsO_4 (Serva, Heidelberg, Germany) for 1 h, dehydrated in ethanol (30–90%) and acetone (90-100%) and embedded in Epon E812 (Roth, Karlsruhe, Germany) polymerized for 24 h at 37°C and 7 days at 65°C. Semithin sections were stained with 1% toluidine blue and used for targeting the cells. Ultrathin sections (40 nm thick) were cut with a diamond knife (Diatome, Bienne, Switzerland) on a Reichert Om U3 ultramicrotome (Leica Microsystems, Vienna, Austria) on copper grids (Sigma-Aldrich; St. Louis, MO, USA) and stained with 1% uranyl acetate (Ted Pella, Inc., Redding, CA, USA) and lead citrate (Ted Pella, Inc., Redding, CA, USA). The material was examined using a JEM 100 CX transmission electron microscope (JEOL, Tokyo, Japan) operating at 60 kV on IMAGO – EM23 film (NDT System, Warsaw, Poland).

Annexin V/propidium iodide (PI) binding assay

To assess the extent of cell death, the Tali Apoptosis kit - Annexin V Alexa Fluor 488 and Propidium Iodide (Invitrogen) was used according to the manufacturer's instructions. In short, after the arsenic trioxide treatment, the cells were collected from 6-well plates using trypsin-EDTA solution, centrifuged at 300 × g for 8 min, resuspended in ABB (annexin binding buffer) and incubated with Annexin V Alexa Fluor 488 at RT in the dark for 20 minutes. Following the centrifugation at 300 × g for 5 min, the cells were again resuspended in ABB and incubated with propidium iodide at RT in the dark for 5 minutes. The cells were analyzed using a Tali Image-Based Cytometer (Invitrogen). The data were quantified by FCS Express Research Edition software (version 4.03; De Novo Software, New Jersey, NJ, USA) and expressed as the percentage of cells in each population (viable Annexin V-/PI-; early apoptotic Annexin V+/PI-; late apoptotic Annexin V+/PI+; necrotic Annexin V-/PI+).

DNA content analysis

For DNA content analysis, the Tali Cell Cycle Kit (Invitrogen) was used according to the manufacturer's instructions. Briefly, the treated cells were harvested from 6-well plates by trypsinization, rinsed with PBS, fixed in ice-cold 70% ethanol at 4°C, and left at -25°C overnight. The cells were then centrifuged at 1000 × g for 5 min at 4°C and washed with PBS the second day. After centrifugation at 500 × g for 10 min at 4°C, the cells were resuspended in Tali Cell Cycle Solution containing propidium iodide (PI), RNase A, and Triton X-100. Following 30-min incubation at RT in the dark, the cells were analyzed using a Tali Image-Based Cytometer (Invitrogen) and the percentage of cells in each phase of the cell cycle was determined using FCS Express Research Edition software (version 4.03; De Novo Software, New Jersey, NJ, USA).

Flow cytometric analysis for cyclin A expression

Cells cultured on 6-well plates were trypsinized, washed and then suspended in PBS. Cells were centrifuged (5 min, 300 x g). The obtained pellet was fixed with Cytofix/Cytoperm Fixation Permeabilization Solution (BD Pharmingen, San Diego, CA, USA), for 30 minutes. The cells were washed with Perm/Wash Buffer (BD Pharmingen, San Diego, CA, USA). Following centrifugation (5 min, 300 x g), the cells were permeabilized with Cytofix/CytopermPlus Permeabilization Buffer (BD Pharmingen, San Diego, CA, USA), and incubated for 10 minutes on ice. The cells were washed with Perm/Wash Buffer, then centrifuged (5 min, 300 x g) and resuspended in Cytofix/Cytoperm Fixation Permeabilization Solution. After 5 minutes, the cells were washed with Perm/Wash Buffer, centrifuged (5 min, 300 x g), incubated for 10 minutes with 0.5% BSA/PBS and again centrifuged. For intracellular staining, the cell suspensions were transferred into flow cytometric tubes containing 20 µl of FITC conjugated mouse anti-human cyclin A (BD Pharmingen, San Diego, CA, USA) and 200 µl of 0.5% BSA. Following a 45-min incubation (4°C, in the dark) and washing with BSA, the cells were centrifuged (5 min, 300 x g) to wash off excess antibody and resuspended in 200 µl of BSA for flow cytometric analysis on a FACScan instrument (Becton-Dickinson, San Jose, CA, USA), with BD CellQuest Pro software Version 5.2.1 (BD Biosciences, San Jose, CA, USA) and with FlowJo 7.5.5 (Tree Star Inc., Ashland, OR, USA).

Quantitative real-time PCR analysis

To determine the expression level of cyclin A, SYBR green-based quantitative real-time PCR was performed using LightCycler 2.0 Instrument (Roche Applied Science; *Mannheim*, Germany) and LightCycler Software Version 4.0. Total RNA from the A549 cells was prepared by using the Total RNA kit (A&A biotechnology; Gdynia, Poland) according to the manufacturer's protocol. The reverse transcription and quantitative PCR reactions were performed in a single 20 *µl* LightCycler capillary (Roche Applied Science; *Mannheim*, Germany) as a one-step real-time qRT-PCR with TranScriba reverse transcriptase and Master Mix SYBR (*TranScriba-qPCR Master Mix SYBR kit; A&A biotechnology; Gdynia, Poland*) as described by the manufacturer. The *total reaction* mixture

(20 µl) *contained 100 ng of* RNA and 1 µM of each primer in addition to the *TranScriba-qPCR Master Mix SYBR kit components. The primers used were as follows: forward, 5'-GTCACATGCTCATCATTTACA-3'; reverse, 5'-GGTACTGAAGTCCGGGAACC-3'. One cycle of reverse transcription* was carried out for 10 min at 50°C, one cycle of denaturation for 3 min at 95°C, and 40 cycles of denaturation for 15 s at 95°C, followed by annealing and elongation for 30 s at 60°C. Relative cyclin A mRNA expression levels were quantified using the comparative threshold cycle (CT) method [22] and the results were normalized to the expression of the housekeeping gene TBP (TATA-binding protein) and presented as a fold difference relative to a calibrator sample (untreated cells).

Fluorescence microscopy

For observations using fluorescence microscopy, A549 cells were briefly washed with PBS, fixed in 4% paraformaldehyde (15 min, RT) and then washed with PBS (3 x 5 min). After that, the cells were incubated in permeabilization solution (0.25% Triton X-100 in PBS) and blocked with 1% BSA. After permeabilization, the cells were incubated with mouse monoclonal anti-cyclin A antibody (Sigma-Aldrich, St. Louis, MO, USA) (60 min, RT), washed three times with PBS and incubated with Alexa Fluor 488 goat anti-mouse IgG (Invitrogen/Life Technologies, Carlsbad, CA, USA) (45 min, RT, in the dark). Nuclear staining was performed with DAPI (Sigma-Aldrich, St. Louis, MO, USA). After incubation, the cells were washed with PBS and then mounted on slides in Aqua Poly/Mount (Polysciences, Warrington, PA, USA). Both cyclin A and DAPI staining were examined using an Eclipse E800 microscope with a Y-FL fluorescence attachment (Nikon), NIS-Elements 3.30 image analysis system and CCD camera (DS-5Mc-U1; Nikon).

Results

Control cells exhibited typical epithelial-like morphology with kidney-shaped or oval nuclei. The cells maintained their adherence to each other. An increasing number of morphological alternations was observed in a dose-dependent manner. After ATO treatment the cells became enlarged and rounded. Vacuolization, chromatin condensation, nucleus shrinkage and loss of adhesion between cells were also characteristic of ATO-treated cells (Fig. 1). At the electron microscope level, alterations in nuclei structure and shape, swollen mitochondria and lysosome-like structures were seen. Giant flattened cells with one big nucleus – which suggested mitotic catastrophe – were observed as well (Fig. 2). Fluorescence microscopic analysis of cyclin A revealed low expression of this protein in the control and ATO-treated cells. In the control cells and cells incubated with 5 µM of ATO, cyclin A expression was observed mainly in the nucleus. With increasing doses of arsenic trioxide, numbers of cells with cytoplasmic expression of cyclin A increased simultaneously, with the protein often localized in the form of cytoplasmic foci (Fig. 3). Real-time PCR analysis showed slightly decreased levels of cyclin A mRNA after treatment with 10 µM and 15 µM of ATO. In turn, the lowest dose of drug did not affect the expression level of cyclin A mRNA (Fig. 4). Expression of cyclin A in A549 cells was too low for flow cytometric analysis (data not shown). Our results showed that arsenic trioxide affected distribution of the cell cycle after 24 h incubation. A statistically significant increase in the percentage of G0/G1 cells was observed after incubation with 5 µM arsenic as compared to the control population, which was followed by decreases in higher doses of the drug. Concomitantly, an inverted tendency resulted from the treatment as regards the G2/M fraction of cells, i.e. decreased percentages at 5 µM ATO were followed by the enriched population at higher concentrations of the agent. The dose of 5 µM also featured a compromised population of S-phase cells. Although the subG1 fraction of cells was reduced as a result of the treatment (Fig. 5), a more in-depth image-based cytometric analysis of apoptosis using annexin V/PI showed rather high resistance of A549 cells to arsenic trioxide. The drug caused only a slight decrease in the number of viable cells, with early and late apoptotic cells constituting only a small percentage of cells. The predominant type of cell death induced in this study was necrosis (Fig. 6).

Discussion

The purpose of anti-tumor therapy is to selectively induce cell death in cancer cells and to save healthy cells to the greatest possible extent. There are several types of cell death, but one of the most well-known is apoptosis. Maintenance of a balance between numbers of proliferating cells and apoptotic cells is essential for proper development of the whole organism. Apoptosis as a physiological process is involved in embryogenesis, development of the immune system, regeneration of tissues, as well as elimination of ageing cells. Apoptosis can be induced in response to external stressors such as UV radiation, cytostatics or toxins of bacterial origin [6]. In this study, A549 cells observed under a transmission-electron microscope showed no changes characteristic for apoptosis such as nuclear condensations, membrane blebbing or presence of apoptotic bodies. Ultrastructural changes induced by 5 µM ATO could indicate mitotic catastrophe, but in contradiction to these expectations, a significant increase in the G2/M phases and polyploidy was not observed. Increasing doses of arsenic trioxide caused subsequent changes – stronger vacuolization of the cytoplasm, nucleus shrinkage and swollen mitochondria. Image-based cytometry analysis showed that A549 cells are resistant to arsenic trioxide in monotherapy. One of the factors determining the ATO resistance in A549 cells may be a high level of glutathione. Han et al. found that arsenic trioxide did not affect free radicals and glutathione levels in A549 cells. Changes in membrane potential in mitochondria were also not observed. All these data suggest that high antioxidative potential exists in A549 cells. In line with this supposition, reducing the glutathione level can be

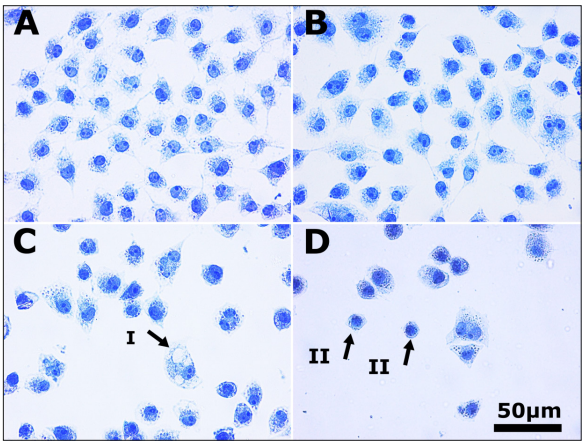

Fig. 1. Effect of arsenic trioxide (ATO) on morphology of A549 cells; **A** – control cells, **B** – cells treated with 5 μM ATO, **C** – cells treated with 10 μM ATO, **D** – cells treated with 15 μM ATO. Bar 50 μm. Enlarged vacuolized cell (I) and shrunken cells (II) were observed

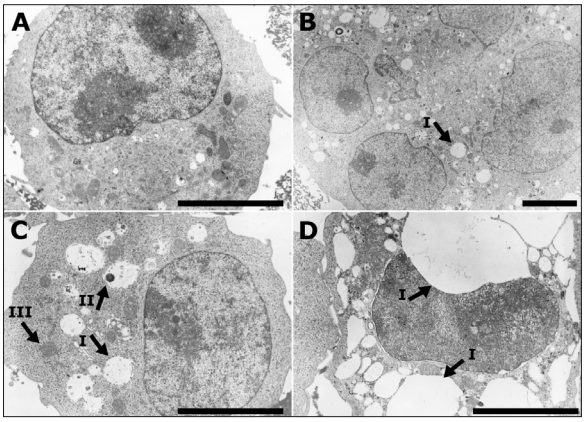

Fig. 2. Ultrastructure of A549 cells treated with arsenic trioxide (ATO); **A** – Control cells, **B** – Cells treated with 5 μM ATO, **C** – Cells treated with 10 μM ATO, **D** – Cells treated with 15 μM ATO. Bar=5 μm. Vacuolization (I), lysosome-like structure (II) and swollen mitochondria (III) were observed

an efficient therapy that makes A549 cells more susceptible to arsenic trioxide. For example, buthionine sulfoximine, a well-known glutathione synthesis inhibitor, exhibited a synergistic effect with clinically achievable doses of arsenic trioxide, causing a decrease in mitochondrial membrane potential, G2/M cell cycle arrest and apoptosis induction in A549 cells [13]. Incorrect expression of cell cycle regulators is characteristic of most cancer cells. Cyclin A localizes predominantly in the nucleus. Transport of cyclin A from the nucleus to the cytoplasm has been proven, but details of this process remain unclear. It is known that cyclin A transport requires binding to its protein partner CDK2. Other studies have shown that CDK2/cyclin A complex is bound to the endoplasmic reticulum in the cytoplasmic space by SCAPER protein (S phase cyclin A-associated protein residing in the endoplasmic reticulum) [16,26]. Moreover, it has been discovered that cyclin A has a domain

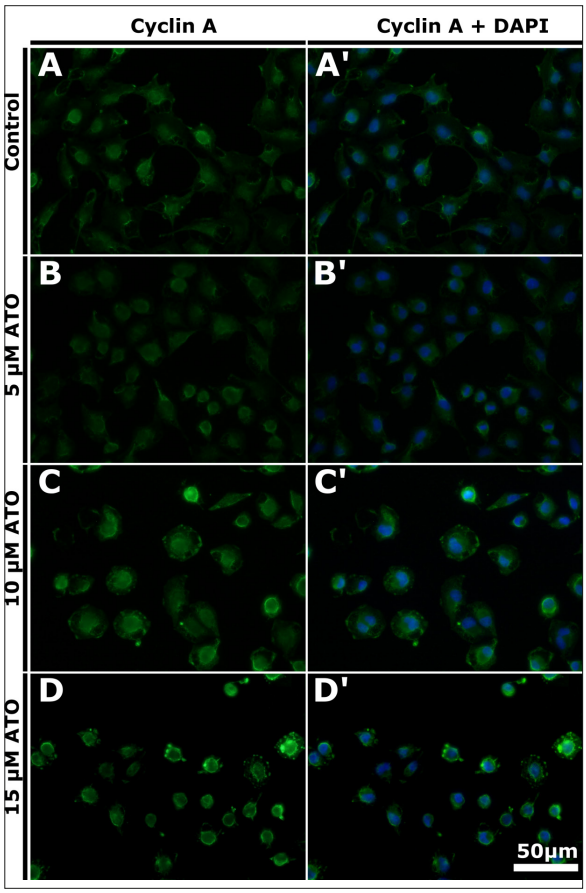

Fig. 3. Fluorescence microscopic examination of cyclin A localization in A549 cells treated with arsenic trioxide (ATO). The cells were treated with 5, 10 and 15 μM ATO and immunolabeled for the presence of cyclin A (**A,B,C,D**). Cell nuclei were stained with DAPI (**A',B',C'D'**). Bar = 50 μm

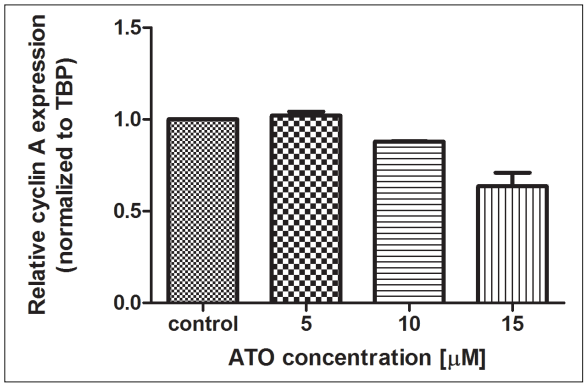

Fig. 4. Real-time PCR analysis of cyclin A mRNA. Relative expression of cyclin A mRNA in A549 cells after treatment with 5, 10 and 15 μM ATO for 24 h. The expression was normalized to TBP and presented as a fold difference relative to a calibrator sample (untreated A549 cells; designated as 1). Results are representative of two independent experiments

which allows binding to the centrosome, and this assembly is essential for proper transition through G2/M phase [25]. Laboratory data suggest that arsenic triox-

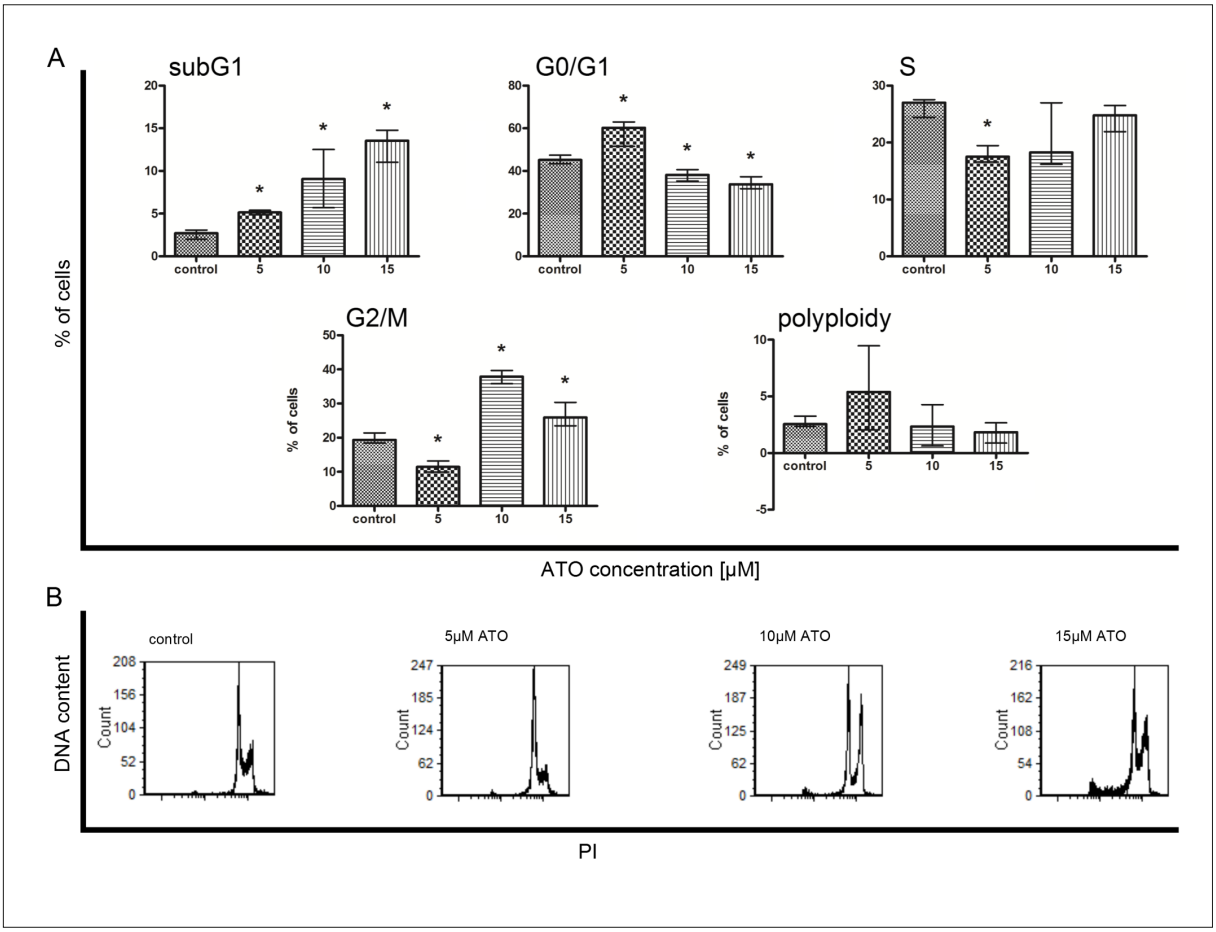

Fig. 5. Image-based cytometry analysis of the cell cycle distribution in A549 cells; **A –** Diagrams for each group defined according to DNA content are shown. Cells with DNA content corresponding to subG1 fraction, G0/G1 phases, S phase, G2/M phases and polyploidy. Columns – median percentage of cells, bars – interquartile range. Asterisks denote statistical significance as compared to control cells (Mann-Whitney U, $p<0.05$). Results are representative of five independent experiments, **B –** Representative histograms of cell cycle phases for each of the ATO doses used

ide is capable of downregulating the expression of cyclin A in cells. In pancreatic cancer cells MiaPaCa-2 and PANC-1 ATO depleted levels of cyclins A, B1 and D1, without an effect on the expression of relevant CDKs [20]. On the other hand, depleted expression of cyclin A may result in increased resistance to apoptosis. Grzanka et al. in their study suggested the involvement of cyclin A in the apoptotic pathway in the K-562 line after treatment with doxorubicin. Along with increasing doses of the drug, and the percentage of apoptotic cells, simultaneous increase in the percentage of cyclin A-positive cells was observed [12]. In agreement with this, silencing of cyclin A expression in leukemia cells caused a decrease in proapoptotic potential of vinca alkaloids [5]. Żuryń et al. also observed an increase in the percentage of cyclin A-positive cells of the HL-60 leukemia line after treatment with doxorubicin and etoposide. An increase in the cytoplasmic pool of cyclin A was also observed [30]. Additionally, cyclin A acts as a negative regulator of RhoA protein, overexpression of which affects cell migration and tumor aggressiveness. Arsic et al. have shown that in fibroblasts with silenced expression of cyclin A, cytoskeletal rearrangements and significant downregulation of RhoA expression take place. These effects have been associated with increased motility and invasiveness of the cells, which suggests the involvement of cyclin A in tumor metastasis. Measurement of cyclin A expression in primary colon carcinoma (SW480) and distant lymph node metastasis (SW620) have shown lower expression of cyclin A in metastatic cells, which confirmed putative cyclin A involvement in metastasis [1]. An increased level of RhoA in lung carcinoma cells is associated with intensified carcinogenesis and proliferation. It has also been proven that inhibition of RhoA activity can be an efficient therapy for non-small cell lung cancer [29]. It seems a reasonable supposition that another mechanism by which arsenic trioxide exerts its cytotoxic effect on the A549 line involves cyclin A and the Rho-ROCK pathway. Probably, in the A549 cells with impaired cyclin A expression, ATO further depletes protein concentration, thus making the cells even more insensitive to apoptotic signals. In our study this putative diminishing influence of ATO on the cyclin A mRNA level was confirmed and shown to be dose-dependent.

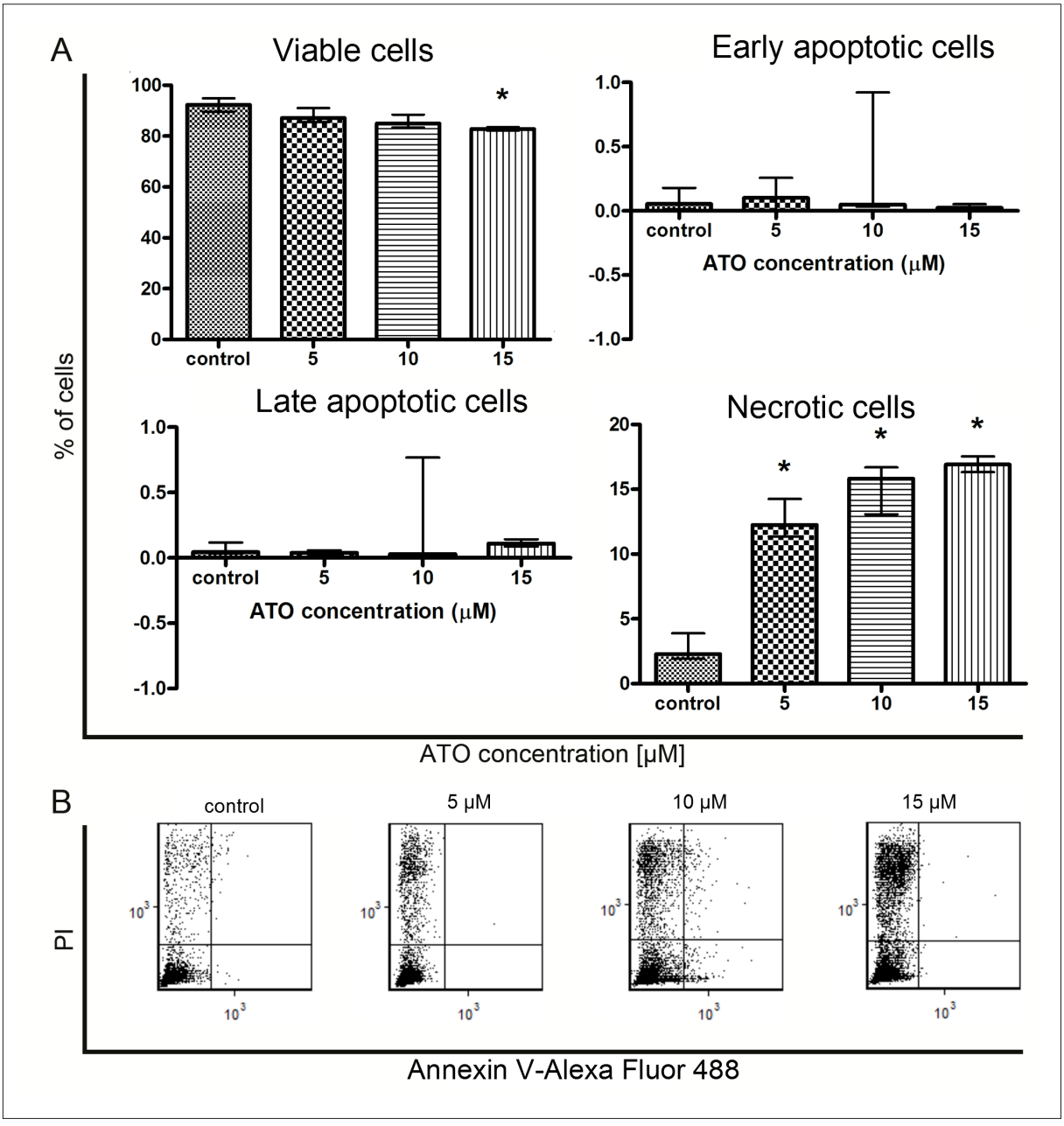

Fig. 6. Image-based cytometry analysis of apoptosis, necrosis and cell viability – annexin V/propidium iodide (PI) assay; **A –** Percentage of viable, early apoptotic, late apoptotic, and necrotic cells. Columns – median percentage of cells, bars – interquartile range. Asterisks denote statistical significance as compared to control cells ($p<0.05$). Results are representative of five independent experiments, **B –** Representative dot plots of annexin V/PI-stained cells for each of the ATO doses used

If this hypothesis is correct, decreased expression of cyclin A may be another factor that determines ATO resistance in A549 cells. Moreover, confirmation of the correlation between cyclin A and ROCK activity in the A549 line may be crucial for establishment of the prognostic value of cyclin A in non-small cell lung cancer. It is noteworthy that in our study arsenic trioxide induced G0/G1 cell cycle arrest. There have been other studies that obtained similar results. Walker et al. observed that arsenic trioxide induces G0/G1 phase arrest in a dose-dependent manner [27]. In contrast, Kim et al. observed no effect of arsenic trioxide on cell cycle distribution in A549 cells [18]. Moreover, it has been reported that arsenic trioxide can induce G2/M arrest in normoxic and hypoxic A549 cells [25]. In our study the G0/G1 phase and G2/M phase arrests were visible, depending on the dose of ATO, which might be related to the alterations in cyclin A regulation. Qi et al. reported that in the A549 cells cell cycle distribution, i.e. G0/G1 phase arrest may correlate with cyclin A expression [24]. This was in good

accord with our results as well, in which G0/G1 arrest was found only at 5 μM ATO, when the cyclin A mRNA level was relatively high as compared to other doses. In our fluorescence reaction, we observed moreover that localization of cyclin A was higher in the nucleus area for the control and 5 μM treated cells, when the G0/G1 block also comprised the most significant fraction of cells, whereas for other concentrations this fraction was compromised and cyclin A was found mainly in the cytoplasm. As cyclin A is degraded in prometaphase cells, its increased cytoplasmic levels and foci formation along with the increased G2/M population of cells may well imply enhanced removal of this protein in our conditions [8]. In conclusion, these data indicate that the effectiveness of arsenic trioxide in the context of cell cycle arrest is determined by the time of exposure and cell culture conditions and may also be associated with cyclin A alterations.

References

[1] Arsic N., Bendris N., Peter M., Begon-Pescia C., Rebouissou C., Gadéa G., Bouquier N., Bibeau F., Lemmers B., Blanchard J.M.: A novel function for Cyclin A2: control of cell invasion via RhoA signaling. J. Cell Biol., 2012; 196: 147-162

[2] Beamish H., de Boer L., Giles N., Stevens F., Oakes V., Gabrielli B.: Cyclin A/cdk2 regulates adenomatous polyposis coli-dependent mitotic spindle anchoring. J. Biol. Chem., 2009; 284: 29015-29023

[3] Cheng J., Wei H.L., Chen J., Xie B.: Antitumor effect of arsenic trioxide in human K562 and K562/ADM cells by autophagy. Toxicol. Mech. Methods, 2012; 22: 512-519

[4] Chibazakura T., Kamachi K., Ohara M., Tane S., Yoshikawa H., Roberts J.M.: Cyclin A promotes S-phase entry via interaction with the replication licensing factor Mcm7. Mol. Cell. Biol., 2011; 31: 248-255

[5] Ehrhardt H., Schrembs D., Moritz C., Wachter F., Haldar S., Graubner U., Nathrath M., Jeremias I.: Optimized anti-tumor effects of anthracyclines plus Vinca alkaloids using a novel, mechanism-based application schedule. Blood, 2011; 118: 6123-6131

[6] Elmore S.: Apoptosis: a review of programmed cell death. Toxicol. Pathol., 2007; 35: 495-516

[7] Foster K.A., Oster C.G., Mayer M.M., Avery M.L., Audus K.L.: Characterization of the A549 cell line as a type II pulmonary epithelial cell model for drug metabolism. Exp. Cell Res., 1998; 243: 359-366

[8] Geley S., Kramer E., Gieffers C., Gannon J., Peters J.M., Hunt T.: Anaphase-promoting complex/cyclosome-dependent proteolysis of human cyclin A starts at the beginning of mitosis and is not subject to the spindle assembly checkpoint. J. Cell Biol., 2001; 153: 137-148

[9] Giard D.J., Aaronson S.A., Todaro G.J., Arnstein P., Kersey J.H., Dosik H., Parks W.P.: *In vitro* cultivation of human tumors: establishment of cell lines derived from a series of solid tumors. J. Natl. Cancer Inst., 1973; 51: 1417-1423

[10] Gong D., Ferrell J.E.Jr.: The roles of cyclin A2, B1, and B2 in early and late mitotic events. Mol. Biol. Cell, 2010; 21: 3149-3161

[11] Gong D., Pomerening J.R., Myers J.W., Gustavsson C., Jones J.T., Hahn A.T., Meyer T., Ferrell J.E.Jr.: Cyclin A2 regulates nuclear-envelope breakdown and the nuclear accumulation of cyclin B1. Curr. Biol., 2007; 17: 85-91

[12] Grzanka A., Żuryń A., Styczyński J., Grzanka A.A., Wiśniewska H.: The effect of doxorubicin on the expression of cyclin A in K-562 leukemia cell line. Neoplasma, 2005; 52: 489-493

[13] Han Y.H., Kim S.Z., Kim S.H., Park W.H.: Induction of apoptosis in arsenic trioxide-treated lung cancer A549 cells by buthionine sulfoximine. Mol. Cells, 2008; 26: 158-164

[14] Huang Y., Sramkoski R.M., Jacobberger J.W.: The kinetics of G2 and M transitions regulated by B cyclins. PLoS One, 2013; 8: e80861

[15] Hukkanen J., Lassila A., Päivärinta K., Valanne S., Sarpo S., Hakkola J. Pelkonen O., Raunio H.: Induction and regulation of xenobiotic-metabolizing cytochrome P450s in the human A549 lung adenocarcinoma cell line. Am. J. Respir. Cell Mol. Biol., 2000; 22: 360-366

[16] Jackman M., Kubota Y., den Elzen N., Hagting A., Pines J.: Cyclin A- and cyclin E-Cdk complexes shuttle between the nucleus and the cytoplasm. Mol. Biol. Cell, 2002; 13: 1030-1045

[17] Kabeche L., Compton D.A.: Cyclin A regulates kinetochore-microtubules to promote faithful chromosome segregation. Nature, 2013; 502: 110-113

[18] Kim J., Lee J.J., Kim J., Gardner D., Beachy P.A.: Arsenic antagonizes the Hedgehog pathway by preventing ciliary accumulation and reducing stability of the Gli2 transcriptional effector. Proc. Natl. Acad. Sci. USA, 2010; 107: 13432-13437

[19] Li L., Wang J., Ye R.D., Shi G., Jin H., Tang X., Yi J.: PML/RARα fusion protein mediates the unique sensitivity to arsenic cytotoxicity in acute promyelocytic leukemia cells: mechanisms involve the impairment of cAMP signaling and the aberrant regulation of NADPH oxidase. J. Cell Physiol., 2008; 217: 486-493

[20] Li X., Ding X., Adrian T.E.: Arsenic trioxide induces apoptosis in pancreatic cancer cells via changes in cell cycle, caspase activation, and GADD expression. Pancreas, 2003; 27: 174-179

[21] Lieber M., Smith B., Szakal A., Nelson-Rees W., Todaro G.: A continuous tumor-cell line from a human lung carcinoma with properties of type II alveolar epithelial cells. Int. J. Cancer, 1976; 17: 62-70

[22] Livak K.J., Schmittgen T.D.: Analysis of relative gene expression data using real-time quantitative PCR and the $2^{-\Delta\Delta C}{}_{T}$ method. Methods, 2001; 25: 402-408

[23] Pascreau G., Eckerdt F., Churchill M.E., Maller J.L.: Discovery of a distinct domain in cyclin A sufficient for centrosomal localization independently of Cdk binding. Proc. Natl. Acad. Sci. USA, 2010; 107: 2932-2937

[24] Qi Y., Tu Y., Yang D., Chen Q., Xiao J., Chen Y., Fu J., Xiao X., Zhou Z.: Cyclin A but not cyclin D1 is essential for c-myc-modulated cell-cycle progression. J. Cell. Physiol., 2007; 210: 63-71

[25] Qu G.P., Xiu Q.Y., Li B., Liu Y.A., Zhang L.Z.: Arsenic trioxide inhibits the growth of human lung cancer cell lines via cell cycle arrest and induction of apoptosis at both normoxia and hypoxia. Toxicol. Ind. Health, 2009; 25: 505-515

[26] Tsang W.Y., Wang L., Chen Z., Sánchez I., Dynlacht B.D.: SCAPER, a novel cyclin A-interacting protein that regulates cell cycle progression. J. Cell Biol., 2007; 178: 621-633

[27] Walker A.M., Stevens J.J., Ndebele K., Tchounwou P.B.: Arsenic trioxide modulates DNA synthesis and apoptosis in lung carcinoma cells. Int. J. Environ. Res. Public Health, 2010; 7: 1996-2007

[28] Wu X., Shi J., Wu Y., Tao Y., Hou J., Meng X., Hu X., Han Y.,

Jiang W., Tang S., Zangari M., Tricot G., Zhan F.: Arsenic trioxide-mediated growth inhibition of myeloma cells is associated with an extrinsic or intrinsic signaling pathway through activation of TRAIL or TRAIL receptor 2. Cancer Biol. Ther., 2010; 10: 1201-1214

[29] Yano Y., Satoh H., Fukumoto K., Kumadaki I., Ichikawa T., Yamada K., Hagiwara K., Yano T.: Induction of cytotoxicity in human lung adenocarcinoma cells by 6-O-carboxypropyl-α-tocotrienol, a redox-silent derivative of α-tocotrienol. Int. J. Cancer, 2005; 115: 839-846

[30] Żuryń A., Grzanka A., Stępień A., Grzanka D., Dębski R., Smoliński D.: Expression of cyclin A in human leukemia cell line HL-60 following treatment with doxorubicin and etoposide: the potential involvement of cyclin A in apoptosis. Oncol. Rep., 2007; 17: 1013-1019

The authors have no potential conflicts of interest to declare.